Research Article

A Combined PMHT and IMM Approach to Multiple-Point Target Tracking in Infrared Image Sequence

Mukesh A. Zaveri,[1] S. N. Merchant,[2] and Uday B. Desai[2]

[1] *Computer Engineering Department, Sardar Vallabhbhai National Institute of Technology, Surat 395007, India*
[2] *SPANN Laboratory, Electrical Engineering Department, Indian Institute of Technology-Bombay, Powai, Mumbai 400076, India*

Data association and model selection are important factors for tracking multiple targets in a dense clutter environment. In this paper, we provide an effective solution to the tracking of multiple single-pixel maneuvering targets in a sequence of infrared images by developing an algorithm that combines a sequential probabilistic multiple hypothesis tracking (PMHT) and interacting multiple model (IMM). We explicitly model maneuver as a change in the target's motion model and demonstrate its effectiveness in our tracking application discussed in this paper. We show that inclusion of IMM enables tracking of any arbitrary trajectory in a sequence of infrared images without any a priori special information about the target dynamics. IMM allows us to incorporate *different dynamic models* for the targets and PMHT helps to avoid the uncertainty about the observation origin. It operates in an iterative mode using expectation-maximization (EM) algorithm. The proposed algorithm uses observation association as missing data.

1. INTRODUCTION

Tracking of multiple moving targets in the presence of clutter has significance in surveillance, navigation, and military application. Various approaches have been proposed for multitarget tracking [1, 2]. The most popular filter used for tracking is the Kalman filter [3–9] because of its simplicity and since it is optimal estimate with linear and Gaussian model assumptions. The performance of a tracking algorithm depends on the data association method used for the observation to track assignment and the model selected to track the movement of a target. For data association, the most common method used is the nearest neighbor (NN) method [1]. The performance of the NN-based data association method degrades in a dense clutter environment. To avoid uncertainty about the origin of observation, joint probabilistic data association filter (JPDAF) and multiple hypothesis tracking (MHT) schemes have been developed [1]. In both these cases, the complexity of the algorithm increases with the increase in the number of observations and the number of targets, as both techniques involve formation and evaluation of all the possible data association events. Maximum likelihood approach and PMHT algorithm have been proposed [10–12], which reduces the complexity. Various versions of the PMHT algorithm have been proposed like turbo PMHT, homothetic PMHT, deflationary PMHT, and augmented multimodel PMHT [13–15]. Different versions of PMHT described above do not incorporate changing target dynamic models for an arbitrary target trajectory, whereas the method proposed in this paper explicitly does so.

Model selection is another problem with target tracking. Using a single filter, it is difficult to track an arbitrary trajectory. The interacting multiple model (IMM) algorithm is one of the most popular algorithms for tracking maneuvering targets because of its relatively simple implementation and its ability to handle complicated dynamics. IMM filtering [16–21], which exploits multiple models, has been used successfully to track maneuvering and nonmaneuvering target simultaneously. It has been well established that in terms of tracking accuracy, the IMM algorithm performs significantly better for maneuvering targets than other types of filters (adaptive single model, input estimation, variable dimension, etc. [1]). The performance comparison between a Kalman filter and the interacting multiple model estimator is carried out for single target tracking [22], and it is reported that an IMM estimator is preferred over a Kalman filter to track the maneuvering target.

2. RELATED WORK AND OUR CONTRIBUTIONS

In this paper, we provide a solution to tracking multiple nonmaneuvering and maneuvering point targets in a sequence of infrared images by combining the PMHT and the IMM approaches [23]. In this combined approach, PMHT is first used to compute the measurement-to-target assignment probabilities and to update the target states for the current scan of measurements, where each target state consists of a collection of states, one for each model in the IMM. The IMM is then used to compute a combined state estimate and error covariance matrix for each target, and to predict forward to the next scan, the collection of states for each target based on a fixed transition probability matrix for the models in the IMM. In the current paper, we explicitly model maneuver as a change in target's motion model. Inclusion of IMM enables tracking of any arbitrary trajectory, and PMHT helps to avoid the uncertainty about the observation origin.

In our approach, only validated observations are used to calculate the observation centroid. Moreover, it uses only observation association as missing data, which simplifies E-step and M-step [24] and consequently, it reduces the complexity of the algorithm in comparison with augmented multimodel PMHT algorithm [15]. In the later case, both observation association and target association are treated as nuisance parameters or missing data, which increases the complexity of the algorithm as it requires to explore all the possible configuration of observation association and target association.

A formulation, where IMM is used with PMHT, has been investigated [25, 26]. It is important to note the basic differences between the proposed algorithm in this paper and the one discussed [25, 26]. First, our methodology which incorporates multiple models in the framework of PMHT is quite different from the one discussed [25, 26]. The IMM-PMHT algorithm [25, 26] is similar to the multimodel PMHT (MPMHT) [25, 26] except that the forward-backward algorithm is replaced by the IMM. In the derivation of the algorithm, the key concern is how to apply the IMM to the Kalman smoother, since the IMM supports only a forward procedure (Kalman filter), and, therefore, the algorithm uses an approximation to obtain the backward probability transition matrix. In our approach, PMHT is first used to compute the measurement-to-target assignment probabilities and to update the target states for the current scan of measurements, where each target state consists of a collection of states, one for each model in the IMM. The IMM is then used to compute a combined state estimate and error covariance matrix for each target, and to predict, forward to the next scan, the collection of states for each target based on a fixed transition probability matrix for the models in the IMM. Second, [25, 26] in order to apply the IMM to the Kalman smoother, an assumption is made that the maneuver mode switching process is a Markov process when going backward, and the backward transition matrix is the same as the usual (forward) transition matrix. Thus, the IMM is done in the regular way except that filtering is replaced by smoothing. In our formulation, we have explicitly modeled maneuver as a change in target's motion model rather than modeling it as an increase in the level of pro-
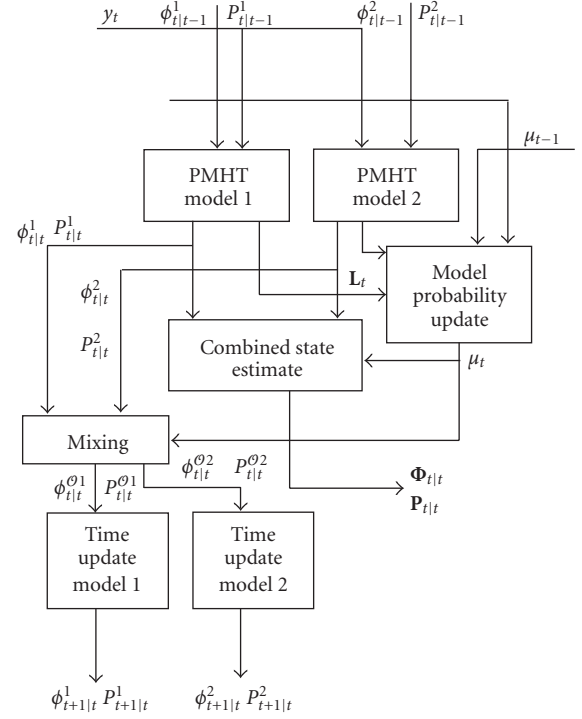

FIGURE 1: PMHT + IMM algorithm for two models.

cess noise; and we clearly demonstrate the effectiveness of such a methodology in our application. Inclusion of IMM enables tracking of any arbitrary trajectory and PMHT helps to avoid the uncertainty about the observation origin. The flow chart of our proposed algorithm, as shown in Figure 1, clearly explains our methodology. Finally, in our approach, only validated observations are used to calculate the observation centroid. Moreover, it uses only observation association as missing data, which simplifies E-step and M-step and consequently, it reduces the complexity of the algorithm in comparison with augmented multimodel PMHT algorithm. In [25, 26], both observation association and target association are treated as nuisance parameters or missing data, which increases the complexity of the algorithm as it requires to explore all the possible configuration of observation association and target association.

For IMM, model probability is to be calculated, which is based on likelihood of the observation and hence needs an assignment of an observation to a target. Earlier IMM-NN, IMM-MHT, IMM-PDAF, and IMM-JPDA ([27–34]) have been used for data assignment. Nevertheless, IMM-NN, IMM-MHT, and IMM-PDAF have the same disadvantages (mentioned earlier) of NN, MHT, and PDAF methods. To reduce the computations, PDA has been replaced by JPDA method with IMM filtering [31, 32]. As pointed out previously, with JPDA, also the complexity increases with the increase in the number of targets and observations.

In our proposed solution, we overcome the above problems by using PMHT approach to calculate the centroid of the observations. This centroid is then used to update the target's state and to evaluate model probabilities. It is important

to note that it does not assign any particular observation to a track. To simplify discussions, our variant of the combination of PMHT and IMM discussed in this paper is named as PMHT + IMM.

3. PROPOSED PMHT + IMM ALGORITHM

In this section, the problem is described in multimodel framework to track arbitrary trajectories of multiple-point targets. The algorithm is divided into two major steps. In the first step, namely, PMHT step, which is based on PMHT algorithm [11], the centroid of the current observation set is calculated for each target. The centroid of the observations is then used to evaluate model likelihood and to update the state for each model. It is followed by an IMM step, which updates the combined state estimate and model probability and predicts the state for the next time instant for each model. It is assumed that the target tracks are independent of each other. From one time instant to another time instant, from observation to observation and from assignment to assignment, independence is assumed. With these assumptions, PMHT algorithm, operating in batch mode [11], can be used with only current set of observations. In the proposed algorithm, there is no need to smooth target state in batch mode, since all calculations are restricted to current time instant only, and consequently, this reduces the complexity of the algorithm.

Let $\mathcal{Y}$ and Φ denote the observation process and the state process, respectively. $\mathbf{Y}^t$ is a set of all observation set for time $t \geq 1$, where t is current time. $\mathbf{Y}_t$ and Φ_t represent the realization of the observation process and the state process at time t. The observation vector

$$\mathbf{Y}_t = (y_t(1), \ldots, y_t(N_o)) \tag{1}$$

represents the received observation vector, where N_o is the number of observations received. Similarly,

$$\Phi_t = (\Phi_t(1), \ldots, \Phi_t(N_t)). \tag{2}$$

Here, N_t is the total number of targets at time instant t, $\Phi_t(s)$ $(1 \leq s \leq N_t)$ represents the combined state vector for target s, and $\phi_t^m(s)$ is the state vector of target s due to model m at time t, where $1 \leq m \leq M$. M is the total number of models used to track that target. To overcome the uncertainty about the observation origin, an assignment process $\mathcal{K}$ is used, and $\mathbf{K}^t$ is a set of all its realizations for time $t \geq 1$. Its realization at time t is denoted by

$$\mathbf{K}_t = (k_t(1), \ldots, k_t(N_o)), \tag{3}$$

where $\mathbf{K}_t$ is an assignment vector and each element of vector $k_t(j) = s$ indicates that target s produces observation j at time t. The observation to track assignment probability Π at time t is given by

$$\Pi_t = (\pi_t(1), \ldots, \pi_t(N_t)). \tag{4}$$

Here, $\pi_t(s)$ indicates the probability that an observation originates from the target s. This probability is independent of the observation, that is,

$$\pi_t(s) = p(k_t(j) = s) \quad \forall j = 1, \ldots, N_o. \tag{5}$$

It is assumed that one observation originates from one target or clutter, which leads to the following constraint on assignment probabilities:

$$\sum_{s=1}^{N_t} \pi_t(s) = 1. \tag{6}$$

Each element of assignment vector $\mathbf{K}_t$ is independent, then the probability of the associated event is

$$p(\mathbf{K}_t) = \prod_{j=1}^{N_o} p(k_t(j)). \tag{7}$$

Finally, the parameter is defined as

$$\mathcal{O} \triangleq (\Phi; \Pi). \tag{8}$$

The assignment vector is treated as missing data and the observation vector as incomplete data, and these together form a complete data set $\mathcal{X} = (\mathcal{Y}, \mathcal{K})$. With the incomplete data formulation, EM algorithm [35, 36] is preferred in obtaining the solution for maximum likelihood (ML) estimate or maximum a posteriori (MAP) estimate of the target state. It consists of two steps: E-step and M-step. E-step evaluates the expectation of log-likelihood of complete data using current assignment probability and current state estimate of target. It estimates assignment probability as a by product. This estimate is used in M-step, which estimates the state of the target by maximizing the log-likelihood functional obtained in E-step.

The estimate of $\mathcal{O} = (\Phi; \Pi)$ at time t is given by Bayes' rule:

$$\begin{aligned} p(\mathcal{O} \mid \mathbf{X}^t) &= p((\Phi_t; \Pi_t) \mid \mathbf{X}_t, \mathbf{X}^{t-1}) \\ &= \frac{p(\mathbf{X}_t \mid (\Phi_t; \Pi_t))}{p(\mathbf{X}_t \mid \mathbf{X}^{t-1})} p((\Phi_t; \Pi_t) \mid \mathbf{X}^{t-1}), \end{aligned} \tag{9}$$

where $p(\mathbf{X}_t \mid \mathbf{X}^{t-1})$ is a normalizing term, and using independence assumption for assignment vector from one time instant to another leads to

$$p((\Phi_t; \Pi_t) \mid \mathbf{X}^{t-1}) = p((\Phi_t; \Pi_t) \mid \hat{\Phi}_{t-1}), \tag{10}$$

where $\hat{\Phi}_{t-1}$ represents the previous estimate;

$$\begin{aligned} &p(\mathcal{O} \mid \mathbf{X}^t) \\ &= \left\{ \frac{p(\mathbf{Y}_t, \mathbf{K}_t \mid (\Phi_t; \Pi_t))}{p(\mathbf{X}_t \mid \mathbf{X}^{t-1})} \right\} \{ (p(\Phi_t; \Pi_t) \mid \hat{\Phi}_{t-1}) \}. \end{aligned} \tag{11}$$

The previous estimate can be used as a priori knowledge. Then MAP estimate of $\mathcal{O}$ is given by

$$\begin{aligned} \hat{\mathcal{O}}_{\mathrm{map}} = \arg \max_{(\Phi_t; \Pi_t)} \big[&\log p(\mathbf{Y}_t, \mathbf{K}_t \mid (\Phi_t; \Pi_t)) \\ &+ \log p((\Phi_t; \Pi_t) \mid \hat{\Phi}_{t-1}) \big]. \end{aligned} \tag{12}$$

Two iterative steps are used to evaluate (12) and the description of the same follows.

(1) Expectation (E-step)

Here, the expectation of the log-likelihood of the completed data is evaluated. Basically, it is an evolution of conditional expectation of $\mathbf{K}_t$ given the observation set $\mathbf{Y}_t$ and the estimated value of $\mathcal{O}$ at pth iteration, $\hat{\mathcal{O}}^{(p)}$;

$$
\begin{aligned}
Q(\mathcal{O} \mid \hat{\mathcal{O}}^{(p)}) &= E\{\log[p(\mathbf{Y}_t, \mathbf{K}_t \mid \mathcal{O})] \mid \mathbf{Y}_t, \hat{\mathcal{O}}^{(p)}\} \\
&= \sum_{\mathbf{K}_t} \log[p(\mathbf{Y}_t, \mathbf{K}_t \mid \mathcal{O})] p(\mathbf{K}_t \mid \mathbf{Y}_t, \hat{\mathcal{O}}^{(p)}).
\end{aligned}
\tag{13}
$$

Independence assumption for each observation and assignment gives,

$$
\begin{aligned}
Q(\mathcal{O} \mid \hat{\mathcal{O}}^{(p)}) &= \sum_{\mathbf{K}_t} \left\{ \sum_{j=1}^{N_o} \log[p(y_t(j) \mid \Phi_t(k(j))) \pi_t(k(j))] \right\} \\
&\times \left\{ \prod_{j=1}^{N_o} p(k_t(j) \mid y_t(j), \hat{\mathcal{O}}^{(p)}) \right\}.
\end{aligned}
\tag{14}
$$

Substituting (5) and summing over all possible configurations of $\mathbf{K}_t$, (14) can be rewritten as

$$
\begin{aligned}
Q(\mathcal{O} \mid \hat{\mathcal{O}}^{(p)}) &= \sum_{s=1}^{N_t} \left[\sum_{j=1}^{N_o} \hat{\mathbf{z}}_t(s, j) \right] \log[\pi_t(s)] \\
&+ \sum_{s=1}^{N_t} \sum_{j=1}^{N_o} \log[p(y_t(j) \mid \Phi_t(s))] \hat{\mathbf{z}}_t(s, j),
\end{aligned}
\tag{15}
$$

where $k_t(j) \in [1, \ldots, N_t]$ and $j \in [1, \ldots, N_o]$. Here, $\hat{\mathbf{z}}_t(s, j)$ represents assignment weights for observation j and target s, and it is defined as

$$
\hat{\mathbf{z}}_t(s, j) = \frac{\pi_t^{(p)}(s) p(y_t(j) \mid \Phi_t^{(p)}(s))}{\sum_{i=1}^{N_t} \pi_t^{(p)}(i) p(y_t(j) \mid \Phi_t^{(p)}(i))}.
\tag{16}
$$

(2) Maximization (M-step)

Using the previous estimate of the state as a priori and the functional obtained in E-step, the estimate of the state is obtained by maximizing

$$
\hat{\mathbf{\Phi}}_t^{(p+1)} = \arg \max_{(\mathbf{\Phi}_t; \Pi_t)} [Q(\mathcal{O} \mid \hat{\mathcal{O}}^{(p)}) + \log p((\mathbf{\Phi}_t; \Pi_t) \mid \hat{\mathbf{\Phi}}_{t-1})]
\tag{17}
$$

with respect to $\pi(s)$ and $\Phi(s)$, $s = 1, \ldots, N_t$, respectively. The value of $Q(\mathcal{O} \mid \hat{\mathcal{O}}^{(p)})$ can be substituted from (15) and the second term of (17) can be written as

$$
p((\mathbf{\Phi}_t; \Pi_t) \mid \hat{\mathbf{\Phi}}_{t-1}) = \left[\prod_{s=1}^{N_t} p(\Phi_0(s)) p(\Phi_t(s) \mid \hat{\mathbf{\Phi}}_{t-1}(s)) \right],
\tag{18}
$$

$$
\begin{aligned}
&\log p((\mathbf{\Phi}_t; \Pi_t) \mid \hat{\mathbf{\Phi}}_{t-1}) \\
&= \sum_{s=1}^{N_t} \{\log[p(\Phi_0(s))] + \log[p(\Phi_t(s) \mid \hat{\mathbf{\Phi}}_{t-1}(s))]\}.
\end{aligned}
\tag{19}
$$

Here, $\Phi(s)$ represents the combined state vector of a target s. So, the parameter $\Phi(s)$ is the set of parameters $(\phi^1(s), \phi^2(s), \ldots, \phi^M(s))$, where $\phi^m(s)$ is the state vector of target s due to model m. Again, each model m is independent of the other m models. It leads to maximization of (17) with respect to $\phi^m(s)$, for $1 \le m \le M$. Maximization of (17) with respect to $\pi(s)$ gives

$$
\pi_t(s) = \frac{1}{N_o} \sum_{j=1}^{N_o} \hat{\mathbf{z}}_t(s, j),
\tag{20}
$$

and with respect to $\Phi(s)$, that is, with respect to $\phi^m(s)$ for each model m ($1 \le m \le M$), it results in Kalman filtering (see the appendix). With Gaussian assumption for a state $\phi_t^m(s)$ ($1 \le m \le M$, $1 \le s \le N_t$), it is given by standard Kalman equations that

$$
\phi_{t|t-1} = f(\phi_{t-1|t-1}) + v_t,
\tag{21}
$$

where v_t represents process noise having covariance Q_p. The observation $y_t(j)$ is given by

$$
y_t = h(\phi_{t|t-1}) + n_t,
\tag{22}
$$

where n_t is an observation noise, assumed to be Gaussian having covariance R.

Now, we describe the PMHT + IMM algorithm with the help of the above formulation. The flow chart for the proposed algorithm using two models for IMM is shown in Figure 1. As the current set of observation $\mathbf{Y}_t$ becomes available, the following two steps are performed at time instant t. The observation set $\mathbf{Y}_t$ is validated using combined state prediction $\Phi_{t|t-1}$ for a given target. PMHT step is evaluated for each target, and for each model of a given target, sequentially. After completion of PMHT step for each target, IMM step is executed.

In the PMHT step, the assignment probabilities and centroid of observations are calculated. These are used by IMM step to update and predict the target state.

(1) PMHT step (PMHT model block in Figure 1).

For each target s ($1 \le s \le N_t$) and for each model m ($1 \le m \le M$):

(a) initialize state $\hat{\phi}_t^m(s) = \hat{\phi}_{t|t-1}^m(s)$ and covariance $P_t^m(s) = P_{t|t-1}^m(s)$ $\hat{\phi}_{t|t-1}^m(s)$ and $P_{t|t-1}^m(s)$ represent previously predicted state and covariance, respectively;

(b) repeat the following steps at each iteration, till error converges to a fixed threshold value, that is, $\|\hat{\phi}_t^{m(p-1)}(s) - \hat{\phi}_t^{m(p)}(s)\| < \epsilon$.

   (i) Calculate the assignment weights for each observation $j = 1, \ldots, N_o$ for each target $i = 1, \ldots, N_t$ using (16).

   (ii) Calculate the assignment probabilities for target s using (20).

   (iii) Calculate the centroid of observations (effective observation):

$$
\begin{aligned}
&y_t^{cm}(s) \\
&= \frac{1}{N_o \pi_t^{m(p+1)}(s)} \sum_{j=1}^{N_o} \hat{\mathbf{z}}_t^{m(p+1)}(s, j) y_t(j).
\end{aligned}
\tag{23}
$$

(iv) Calculate the effective observation noise covariance matrix:

$$R_t^{cm}(s) = \frac{R_t^m(s)}{N_o \pi_t^{m(p+1)}(s)}. \tag{24}$$

(v) State and state covariance updates:

$$\tilde{y} = y_t^{cm}(s) - H_t^m(s)\hat{\phi}_t^{m(p)}(s),$$
$$S^m(s) = H_t^m(s)P_t^{m(p)}(s)(H_t^m(s))^T + R_t^{cm}(s), \tag{25}$$

likelihood of model[1]: $\mathcal{L}^m(s) = \mathcal{N}[\tilde{y}; 0, S^m(s)]$;

$$K_g^m(s) = P_t^{m(p)}(s)(H_t^m(s))^T(S^m(s))^{-1},$$
$$\hat{\phi}_t^{m(p+1)}(s) = \hat{\phi}_t^{m(p)}(s) + K_g^m(s)\tilde{y},$$
$$P_t^{m(p+1)}(s) = P_t^{m(p)}(s) - K_g^m(s)S^m(s)(K_g^m(s))^T. \tag{26}$$

At the end of PMHT step for each target s, for each model m updated state $\hat{\phi}_{t|t}^m(s)$ and updated covariance, $P_{t|t}^m(s)$ are obtained.

(2) IMM step: for each target s ($1 \le s \le N_t$), repeat the following steps.

(a) Model probability update (model probability update block in Figure 1):
for each model $m = 1, \ldots, M$, calculate the model probability using

$$\mu_t^m(s) = \frac{\mu_{t|t-1}^m(s)\mathcal{L}^m(s)}{\sum_{i=1}^M \mu_{t|t-1}^i(s)\mathcal{L}^i(s)}. \tag{27}$$

(b) Combined state and state covariance updates (combined state estimate block in Figure 1):

$$\hat{\Phi}_{t|t}(s) = \sum_{m=1}^M \hat{\phi}_{t|t}^m(s)\mu_t^m(s),$$
$$P_{t|t}(s) = \sum_{m=1}^M \Big[P_{t|t}^m(s) + (\hat{\Phi}_{t|t}(s) - \hat{\phi}_{t|t}^m(s))$$
$$\cdot (\hat{\Phi}_{t|t}(s) - \hat{\phi}_{t|t}^m(s))^T \Big]\mu_t^m(s). \tag{28}$$

(c) For each model $m = 1, \ldots, M$, calculate the following.

(i) Model-conditional initialization (mixing) (mixing block in Figure 1):

$$\hat{\phi}^{0m} = \sum_{i=1}^M \hat{\phi}_{t|t}^i(s)\mu^{i|m},$$
$$P^{0m} = \sum_{i=1}^M \Big[P_{t|t}^i(s) + (\hat{\phi}^{0m} - \hat{\phi}_{t|t}^i(s))$$
$$\cdot (\hat{\phi}^{0m} - \hat{\phi}_{t|t}^i(s))^T \Big]\mu^{i|m}, \tag{29}$$

where

$$\mu^{i|m} = \frac{\xi_{im}^s \mu_t^i(s)}{\mu_{t+1|t}^m}, \qquad \mu_{t+1|t}^m = \sum_{i=1}^M \xi_{im}^s \mu_t^i(s). \tag{30}$$

Here ξ_{im} is the transition probability.

(ii) State and state covariance prediction (time update model block in Figure 1):

$$\hat{\phi}_{t+1|t}^m(s) = F_t^m(s)\hat{\phi}^{0m},$$
$$P_{t+1|t}^m(s) = F_t^m(s)P^{0m}(F_t^m(s))^T + Q_t^m(s). \tag{31}$$

(d) Combined state and state covariance prediction:

$$\hat{\Phi}_{t+1|t}(s) = \sum_{m=1}^M \hat{\phi}_{t+1|t}^m(s)\mu_{t+1|t}^m(s),$$
$$P_{t+1|t}(s) = \sum_{m=1}^M \Big[P_{t+1|t}^m(s) + (\hat{\Phi}_{t+1|t}(s) - \hat{\phi}_{t+1|t}^m(s)),$$
$$(\hat{\Phi}_{t+1|t}(s) - \hat{\phi}_{t+1|t}^m(s))^T \Big]\mu_{t+1|t}^m(s). \tag{32}$$

The transition probability is initialized as

$$\Xi = \begin{bmatrix} 0.998 & 0.001 \\ 0.001 & 0.998 \end{bmatrix} \tag{33}$$

and initial model probability is set to $\mu = \{0.5\ 0.5\}$. Initial model probability for both models is set equally. These parameters are chosen based on the study reported in the literature and our exhaustive experimental investigations. The transition probability matrix is initialized based on the following observation. The diagonal entries of the probability matrix are related to the individual target dynamic models used for tracking. Generally, the target dynamics is consistent and therefore, it has a high probability that it will remain in the same state. So, these diagonal entries are initially set to high values. The nondiagonal entries represent the probabilities of switching between different dynamic models associated with a target. In general, there is a low probability that the target dynamics will change its state, that is, it will switch from one target dynamic model to another, and consequently, the nondiagonal entries are initially set to low values. Similarly, the model probabilities are also initialized with equal probabilities. But, during the execution of algorithm the model probabilities are updated automatically.

4. SIMULATION RESULTS

Synthetic IR images were generated using real-time temperature data [37]. Intensity at different points in images is a function of temperature, surface properties, and other environmental factors. Based on exhaustive empirical study, we have validated the close resemblance between synthetic IR images and real IR images in airborne applications. Due to the classified nature of the real IR images which we used for our investigation, we are limited here to present our results only for synthetic IR images.

---

[1] Note: likelihood of a model is calculated during the first iteration only for given model and target.
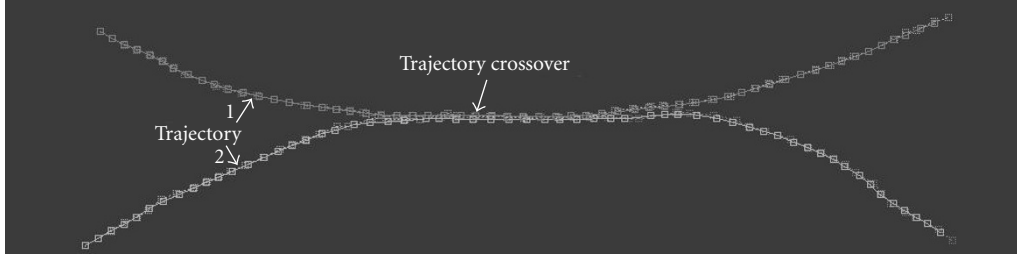
FIGURE 2: Trajectory using SMM-PMHT model for ir44 clip :: crossover.
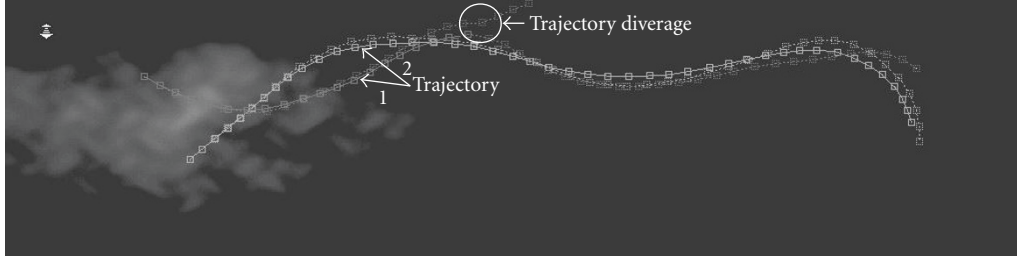

FIGURE 3: Trajectory using CA-PMHT model for ir50 clip.

For simulation, the generated frame size is 1024×256 with a large target movement of ± 20 pixels per frame. Many video clips are simulated with different types of trajectories to evaluate the performance of the proposed algorithm. Two sets of clips have been generated: (i) the first clip set consisting of maneuvering trajectories is generated using B-splines, and it is quite important to note that these generated trajectories do not follow any specific model; (ii) for the second clip set, mixed trajectories are generated using constant acceleration model for non-maneuvering trajectories and cosine and sine functions for nonlinear (maneuvering) trajectories. The second case allows one to generate trajectories with known models and known set of parameters to evaluate the performance of the proposed algorithm. The nonlinear function gives x and y positions of the target at each time t. Extensive simulations have been done and simulation results for a few of the clips from these two different sets are described here. It is assumed that each input clip is processed with the target detection algorithm described in [38, 39]. At each time instant, the output from the detection module is treated as the observation set. As the tracking is done in an image clip, the observation consists of x and y positions only. For our case, t is discrete and also represents the frame number in an image clip. In general, the nonlinear functions are of the following forms:

$$
\begin{aligned}
x(t) &= \alpha^t + A * \text{tri\_fun}(wt), \\
y(t) &= B + A * \text{tri\_fun}(wt),
\end{aligned}
\tag{34}
$$

where tri_fun may be cosine or sine function α takes value less than 1.0, and w is in radians.

Different values for the noise covariances are used:

(i) for the process and the observation to generate trajectories and (ii) for the models used in tracking. This facilitates the simulation of mismatch models, and thereby providing realistic trajectories to evaluate different tracking algorithms. For generating the nonmaneuvering and maneuvering trajectories, the process noise variance and observation noise variance for the position are set to 5.0 and 2.0. The process noise variance value, for both the velocity and the acceleration of the target in case of nonmaneuvering trajectories, is set to 0.001. In our simulations, we have used constant acceleration (CA) and Singer's maneuver model [40] (SMM) for IMM. Both models have six state parameters, namely, position, velocity, and acceleration for x and y. For tracking purposes, in our simulations, the model observation noise variance for the position is set to 9.0 for both models. For all trajectories, the tracking filters are initialized using positions of the targets in the first two frames.

First, we have experimented with only CA (CA-PMHT) and only SMM (SMM-PMHT) algorithms, that is, approach proposed [14] for batch mode length set to 1, for different trajectories in IR clips. Figure 2 represents the tracked trajectories in an IR image clip using one particular type of model, that is, SMM. It shows a crossover of trajectories and fails to track the targets. Figure 3 depicts the failure of CA model to track a target. But our proposed PMHT + IMM method is able to track the target for these IR clips as shown in Figures 4 and 5, respectively. In Figures 2–9, the real trajectory is shown with a solid line, whereas the predicted trajectory is shown using a dotted line.

Figures 6 and 7 present results for target tracking in clutter using the proposed method. It is important to note that for the same IR clips, both CA-PMHT and SMM-PMHT fail to track the targets simultaneously.

Figure 8 represents the variation with time in the likelihood of a model and consecutively the model probability, for different trajectories for the clip ir50 with 0.03% clutter,
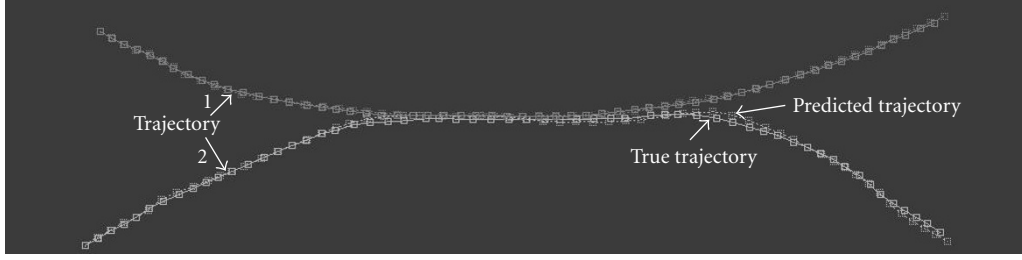
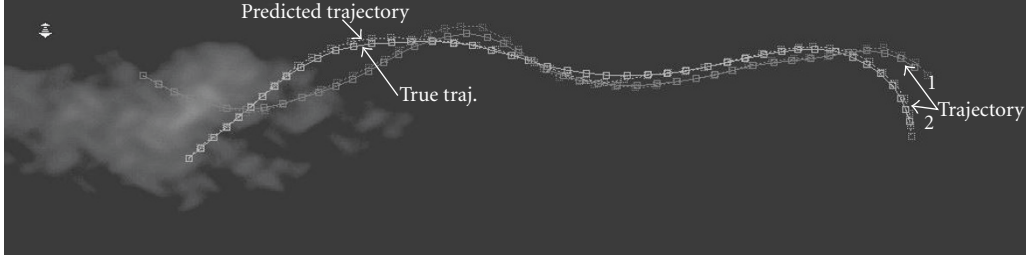Figure 4: Trajectory using PMHT + IMM model for ir44 clip at frame number 57.

Figure 5: Trajectory using PMHT + IMM model for ir50 clip at frame number 44.

respectively. Actually, it depicts the likelihood of a model for a given target and matches with the result obtained for ir50 clip in Figure 7. These results lead to a conclusion that using our proposed PMHT + IMM algorithm, it is possible to track arbitrary trajectories.

Figure 9 represents the result of the proposed tracking algorithm for clip in31_2, which contains 6 targets. Using the proposed PMHT + IMM approach, mean error in position is depicted in Table 1. Table 1(a) compares the results obtained using PMHT with only CA (CA-PMHT) and only SMM (SMM-PMHT) algorithms, that is, approach proposed [14] for batch mode length set to 1, for different trajectories in different infrared image clips. We have also tested the proposed algorithm to track multiple-point target in image clips with different clutter levels. For all trajectories, filters are initialized using positions of the targets in the first two frames. For example, 0.02% clutter level in an image frame represents 0.02% number of pixels of the total pixels in an image to be noisy. "Traj." indicates trajectory number in an image clip. In Table 1, PMHT + IMM represents combined mean error in a position.

For clips ir49 and ir50 in Table 1(a), mean error in position using SMM-PMHT approach [14] is less compared to that of using PMHT + IMM approach. Such a result is expected if only one particular model represents the trajectory quite accurately. For clips ir44 and ir50 in Table 1(a) and ir44, ir49, and ir50 in Table 1(b) with different clutter level, only PMHT + IMM method is able to track both trajectories simultaneously. Therefore, in a scenario where there is no a priori information available about the model for a trajectory, we advocate that the most preferred approach is PMHT + IMM.

Results of the investigations reported [25, 26] indicate that the performance of homothetic (multiple model)

Table 1: Mean Prediction Error in Position.

(a) Without clutter

Traj.	CA-PMHT	SMM-PMHT	PMHT + IMM
		ir44	
1	1.9650	Fails	1.8523
2	3.4995	Fails	3.3542
		ir49	
1	4.9959	1.9257	3.2662
2	5.1730	2.1353	3.0113
		ir50	
1	Fails	2.3164	3.0710
2	5.7795	2.1093	3.1088

(b) With clutter

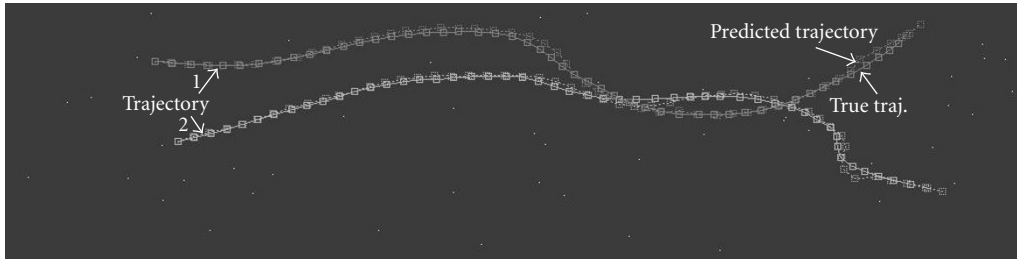| Traj.	PMHT + IMM	
	ir44	
—	0.02%	0.03%
1	2.2849	2.6126
2	Fails	Fails
	ir49	
—	0.02%	0.03%
1	3.4328	3.7474
2	3.1441	5.2833
	ir50	
—	0.02%	0.03%
1	3.3201	3.3174
2	3.6560	3.7897

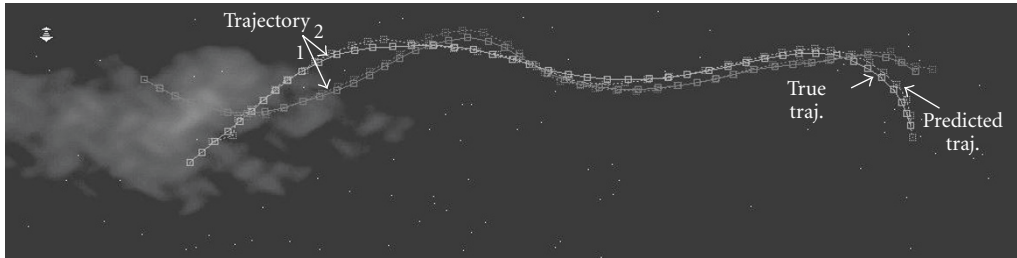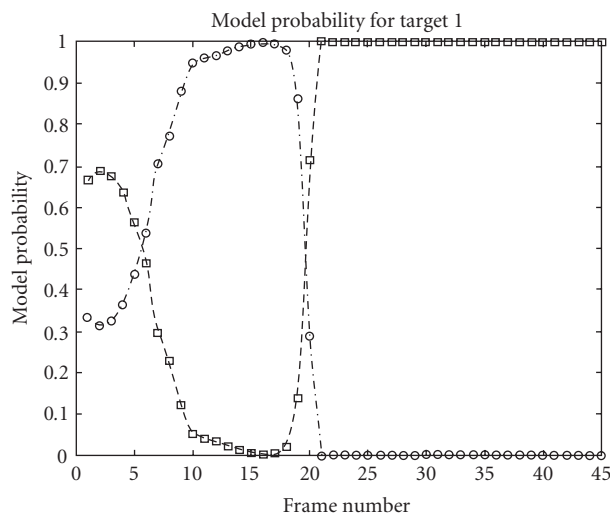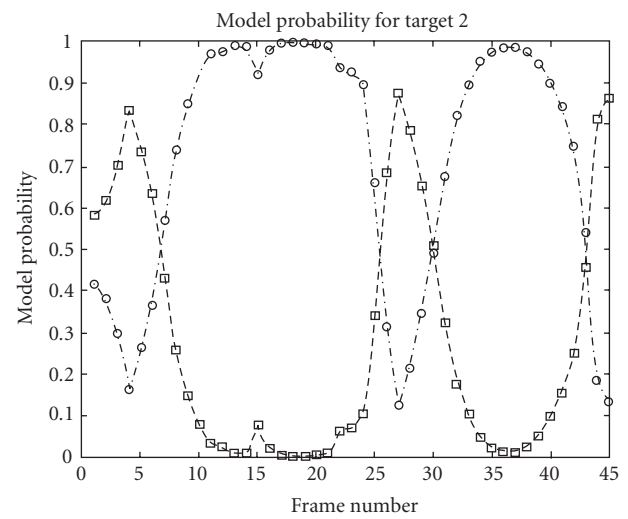Figure 6: Target trajectories for ir49 clip with clutter level 0.02% at frame number 49.

Figure 7: Target trajectories for ir50 clip with clutter level 0.03% at frame number 44.

(a)

(b)

Figure 8: Model probability (ir50 clip with clutter level 0.03%).

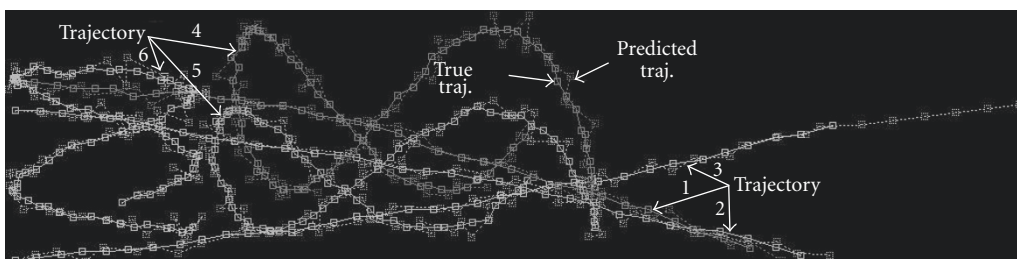

Figure 9: Target Trajectories for in31_2 clip at frame number 79.

PMHT is better than the version of IMM-PMHT discussed [25, 26]. Therefore, we have also experimented using homothetic (multiple model) PMHT [25, 26] for batch mode length set to 1. From the results of our investigation, it is observed that by using maneuvering models based on different process noise covariance values only, it is difficult to track multiple arbitrary trajectories. These results are depicted in Figures 10 and 11 for clip n16. In the first case, we used two constant acceleration models with different noise covariance values, and it fails to track all the targets simultaneously (Figure 10). Whereas in the second case, we used two Singer's models with different noise covariance values and again it fails to track all the targets in the clip. But our proposed approach, namely, PMHT + IMM, is able to track all the targets successfully which are depicted in Figure 12. From the results of this investigation, a reasonable conclusion is that it is not sufficient to model maneuver as a change in the process noise alone, and that improved performance can be obtained on inclusion of the change in target's motion model.

In order to demonstrate the efficacy of our proposed algorithm, we have experimented with a large number of targets, that is, 40 targets in a clip. Figure 13 represents the tracking results for one such clip, namely, ip24 clip. From Figure 13, it is clear that our proposed algorithm is also effective in tracking all the targets successfully in a dense environment, that is, in the presence of a large number of targets. It is also important to note that the parameters for the tracking filters are set to the same value as those set for the clips with few targets. These parameters are process noise variance, observation noise variance and validation gate of size 28×28, and so forth. It is obvious that with such a large validation gate and a large number of targets, the data association problem is very crucial and needs an efficient algorithm. The proposed algorithm performs data association successfully with this set of values. We have performed exhaustive empirical study for a large number of clips with 40 targets. Due to space limitation, it is not possible to include them in the manuscript. We also performed Monte Carlo simulations with a different set of trajectory sets to evaluate the performance of the proposed PMHT + IMM algorithm. Fifty simulations are performed for a given set of trajectories. The process noise covariance and observation noise covariance are set to 0.2 and 2.0, respectively, for trajectory generation. The number of clutter is assumed to be Poisson distributed. The size of clutter window is 10×10 around the actual observed target position. The average number of clutter that falls inside the clutter window is set to 1.

For one of the trajectory sets, the details are as follows. The trajectory set consists of three trajectories. (a) The first is a constant acceleration trajectory with initial position, velocity, and acceleration set to (70, 70), (20, 3), and (0.5, 0.5), and it exists for 22 frames. (b) The second trajectory is generated using constant velocity model and exists for 30 frames. The initial X-Y position and velocity are set to (70, 200) and (20, -3). (c) The third trajectory is of "MIX" type and exists for 70 frames. The initial position and velocity are set to (30, 30) and (10, 1). The target travels with constant velocity from frame 1 to frame 15. It takes three turns: (i) 15° per second from frame 16 to frame 27, (ii) −15° per second from frame

36 to 47, and (iii) 12° per second from frame 58 to frame 68. Then, the target has acceleration of (0.02, 0.02) in X-Y. The true trajectory plot is shown in Figure 14. The prediction and estimation error plot for the third trajectory (MIX type) are depicted in Figures 16 and 15.

To test the bias of the state estimate, we follow the statistical method described in [41]. For this, an estimation error for each component of the state vector is tested individually. Under the hypothesis that the state estimation is unbiased, and assuming that the error is normally distributed each component, indexed by subscript j, is also normally distributed:

$$e(j) = \tilde{\Phi}_{t|t}^{j} \sim \mathcal{N}\left[0, P_{t|t}^{jj}\right], \tag{35}$$

where $\tilde{\Phi}_{t|t}^{j}$ is an estimation error in jth component of the state vector. Each component of the state error is divided by its standard deviation which makes it (under ideal conditions) $\mathcal{N}(0, 1)$, which is also evident from Figure 15.

5. CONCLUSION

Results of our investigation clearly demonstrate the effectiveness of combining PMHT with IMM for the tracking of multiple single-pixel maneuvering targets in sequences of infrared images in a dense cluttered environment. We also conclude that modeling maneuver as a change in targets' motion model could provide enhanced performance compared to modeling it as an increase in the level of process noise. From the simulation results, it is also concluded that the developed method combining PMHT and IMM, with the inclusion of IMM based on only two filters, namely, CA and SMM, performs very well in the application discussed in this paper. The proposed algorithm uses the centroid of observations for state update and prediction. It avoids implicit observation to track assignment and hence there is no ambiguity about the origin of an observation, thereby resolving data association problem. Moreover, the proposed approach is able to track an arbitrary trajectory by incorporating multiple target dynamic models, in the presence of the dense clutter without using any a priori information about the target dynamics.

APPENDIX

Optimal estimate for $\hat{\Phi}_{t}^{(p+1)}$ can be obtained using (17):

$$\hat{\Phi}_{t}^{(p+1)} = \arg \max_{(\Phi_{t}; \Pi_{t})} \left[Q(\mathcal{O} \mid \hat{\mathcal{O}}^{(p)}) + \log p((\Phi_{t}; \Pi_{t}) \mid \hat{\Phi}_{t-1}) \right] \tag{A.1}$$

by taking derivative of $Q(\mathcal{O} \mid \hat{\mathcal{O}}^{(p)})$ and $\log p((\Phi_{t}; \Pi_{t}) \mid \hat{\Phi}_{t-1})$ with respect to $\pi(s)$ and $\Phi(s)$, $s = 1, \ldots, N_{t}$ and equating to zero. Targets are assumed to be independent of each other. The first term in (17) is obtained from E-step using
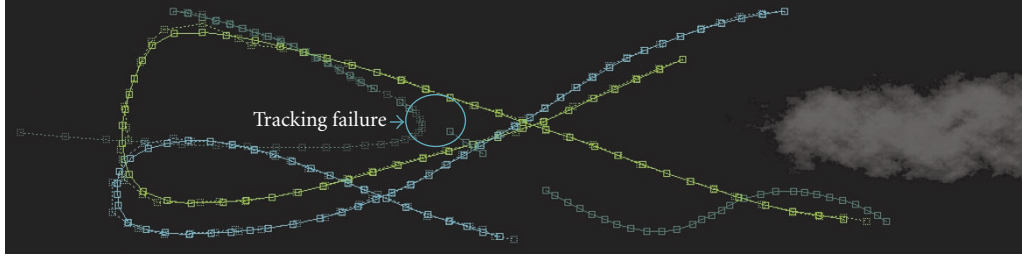
FIGURE 10: n16 clip: tracking with two CA models based on different process noise covariance values [25, 26].

FIGURE 11: n16 clip: tracking with two SMM models based on different process noise covariance values [25, 26].
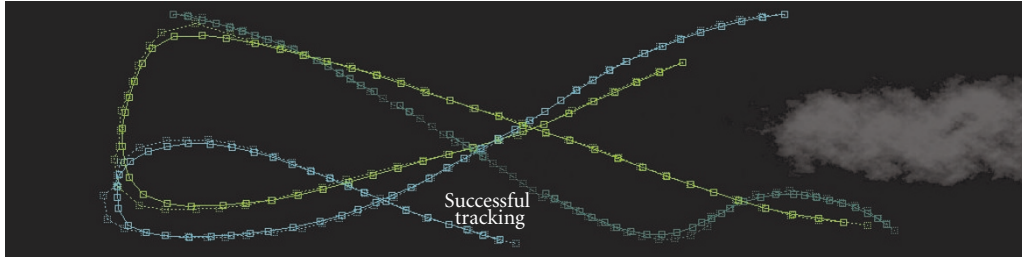

FIGURE 12: n16 clip: tracking with our proposed PMHT + IMM approach.

(15). The maximization of $Q(\mathcal{O} \mid \hat{\mathcal{O}}^{(p)})$ with respect to $\pi(s)$ results into (20). Maximization with respect to $\Phi(s)$ leads to

$$
\nabla_{\Phi(s)} Q(\mathcal{O} \mid \hat{\mathcal{O}}^{(p)})
$$
$$
= \sum_{s=1}^{N_t} \left\{ \nabla_{\Phi(s)} \sum_{j=1}^{N_o} \log \left[p(y_t(j) \mid \Phi_t(s)) \right] \hat{\mathbf{z}}_t(s, j) \right\} = 0,
$$
$$
\text{(A.2)}
$$

where $p(y_t(j) \mid \Phi_t(s))$ is assumed to be Gaussian and written as

$$
p(y_t(j) \mid \Phi_t(s))
$$
$$
= \frac{1}{\sqrt{2\pi|R|}} \exp\{-([y_t(j) - h(\Phi_t(s))]^T R^{-1}[y_t(j) - h(\Phi_t(s))])\},
$$
$$
\text{(A.3)}
$$

where R is observation noise covariance matrix. Then, (A.2) can be written as

$$
\sum_{s=1}^{N_t} \left\{ \nabla_{\Phi(s)} \sum_{j=1}^{N_o} \left[\log \frac{1}{\sqrt{2\pi} \mid R \mid} \right. \right.
$$
$$
\left. \left. - [y_t(j) - h(\Phi_t(s))]^T R^{-1}[y_t(j) - h(\Phi_t(s))] \right] \hat{\mathbf{z}}_t(s, j) \right\}
$$
$$
= \sum_{s=1}^{N_t} \left\{ \nabla_{\Phi(s)} \sum_{j=1}^{N_o} [- [y_t(j) \right.
$$
$$
\left. - h(\Phi_t(s))]^T R^{-1}[y_t(j) - h(\Phi_t(s))]] \hat{\mathbf{z}}_t(s, j) \right\} = 0.
$$
$$
\text{(A.4)}
$$

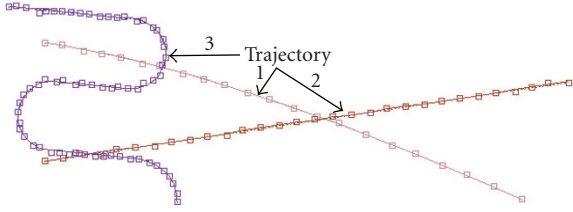Figure 13: ip24 clip: tracking with our proposed PMHT + IMM approach.

Figure 14: True trajectory plot for Monte Carlo simulation.

Let exponent

$$
\begin{aligned}
[y_t(j) - h(\Phi_t(s))]^T R^{-1} [y_t(j) - h(\Phi_t(s))] \\
= f(\Phi_t) = f(\phi_t^1, \ldots, \phi_t^M),
\end{aligned}
\tag{A.5}
$$

where $\Phi_t(s)$ is combined state vector of a target s. Each model is also assumed to be independent of the other models and hence state vector due to each model $\phi_t^m(s)$ is also independent of the other state vectors. For optimal estimate, derivative of a function $f(\Phi_t(s)) = f(\phi_t^1, \ldots, \phi_t^M)$ with respect to Φ_t leads to a derivative with respect to each ϕ_t^m $(1 \le m \le M)$ due to independence assumption of each model and it results into an estimate of $\hat{\phi}_t^m(s)$, which can be obtained by solving

$$
\hat{\phi}_t^{m(p+1)}(s) = \arg\min_{\phi_t^m} [y_t^c - h(\phi_t^m)]^T R_t^{c(-1)} [y_t^c - h(\phi_t^m)],
\tag{A.6}
$$

where y_t^c and R_t^c are effective observation and effective observation covariance matrix, respectively, as described in (23) and (24). Equation (A.6) represents approximated solution to the exact solution which may be messy due to the term $w_t(s, j)$.

MAP estimate of $\hat{\Phi}_t^{(p+1)}$ can be obtained using a priori information about state, that is, the second term in (17). Using an independence assumption for each target, a second term $\log p((\Phi_t; \Pi_t) \mid \hat{\Phi}_{t-1})$ in (17) can be written as in (19):

$$
\begin{aligned}
&\log p((\Phi_t; \Pi_t) \mid \hat{\Phi}_{t-1}) \\
&= \sum_{s=1}^{N_t} \{ \log [p(\Phi_0(s))] + \log [p(\Phi_t(s) \mid \hat{\Phi}_{t-1}(s))] \}.
\end{aligned}
\tag{A.7}
$$

Assumption of each model being independent of the other assumptions leads to

$$
\begin{aligned}
&\log p((\Phi_t; \Pi_t) \mid \hat{\Phi}_{t-1}) \\
&= \sum_{s=1}^{N_t} \left\{ \log \left[\prod_{m=1}^{M} p_{\phi^m}(\phi_0(s)) \right] + \log \left[\prod_{m=1}^{M} p_{\phi^m}(\phi_t(s) \mid \hat{\phi}_{t-1}(s)) \right] \right\} \\
&= \sum_{s=1}^{N_t} \left\{ \sum_{m=1}^{M} p_{\phi^m}(\phi_0(s)) + \sum_{m=1}^{M} p_{\phi^m}(\phi_t(s) \mid \hat{\phi}_{t-1}(s)) \right\},
\end{aligned}
\tag{A.8}
$$

where $p_{\phi^m}(\phi_0(s))$ represents PDF of model m for target s at time $t = 0$. Each $\phi^m(t)$ is also assumed to be Gaussian distributed and written as

$$
\begin{aligned}
&p_{\phi^m}(\phi_t \mid \hat{\phi}_{t-1}) \\
&= \frac{1}{\sqrt{2\pi |P_{t|t-1}|}} \exp \{ - [(\phi_t - \hat{\phi}_{t|t-1})^T P_{t|t-1}^{-1} (\phi_t - \hat{\phi}_{t|t-1})] \}.
\end{aligned}
\tag{A.9}
$$

With an independence assumption for each model and taking a derivative of the term $\log p(\Phi_t(s) \mid \hat{\Phi}_{t-1}(s))$ with respect to $\Phi_t(s)$, it is written as

$$
\begin{aligned}
&\nabla_{\Phi_t(s)} [\log p(\Phi_t(s) \mid \hat{\Phi}_{t-1}(s))] \\
&= \nabla_{\Phi_t(s)} \left[\sum_{s=1}^{N_t} \log \left\{ \prod_{m=1}^{M} p_{\phi^m}(\phi_t(s) \mid \hat{\phi}_{t-1}(s)) \right\} \right] \\
&= \nabla_{\Phi_t(s)} \left[- \left\{ \sum_{s=1}^{N_t} \sum_{m=1}^{M} [(\phi_t^m(s) - \hat{\phi}_{t|t-1}^m(s))^T \right. \right. \\
&\qquad\qquad\qquad \left. \left. \times P_{t|t-1}^{(-1)m}(s)(\phi_t^m(s) - \hat{\phi}_{t|t-1}^m(s))] \right\} \right] \\
&= - \left\{ \sum_{s=1}^{N_t} \sum_{m=1}^{M} \nabla_{\phi_t^m(s)} [(\phi_t^m(s) - \hat{\phi}_{t|t-1}^m(s))^T \right. \\
&\qquad\qquad\qquad \left. \times P_{t|t-1}^{(-1)m}(s)(\phi_t^m(s) - \hat{\phi}_{t|t-1}^m(s))] \right\}.
\end{aligned}
\tag{A.10}
$$

Now, $\hat{\Phi}_t$ is estimated using (A.4) and (A.10), that is, maximization of (17) with respect to $\Phi_t(s)$ results into MAP estimate of a state for model m, $\phi_t^m(s)$, and can be obtained by

$$
\begin{aligned}
\hat{\phi}_t^{(p+1)} = \arg\min_{\phi_t} &[(\phi - \hat{\phi}_{t|t-1})^T P_{t|t-1}^{-1} (\phi - \hat{\phi}_{t|t-1}) \\
&+ [y_t^c - h(\phi_t)]^T R^{c(-1)} [y_t^c - h(\phi_t)]]
\end{aligned}
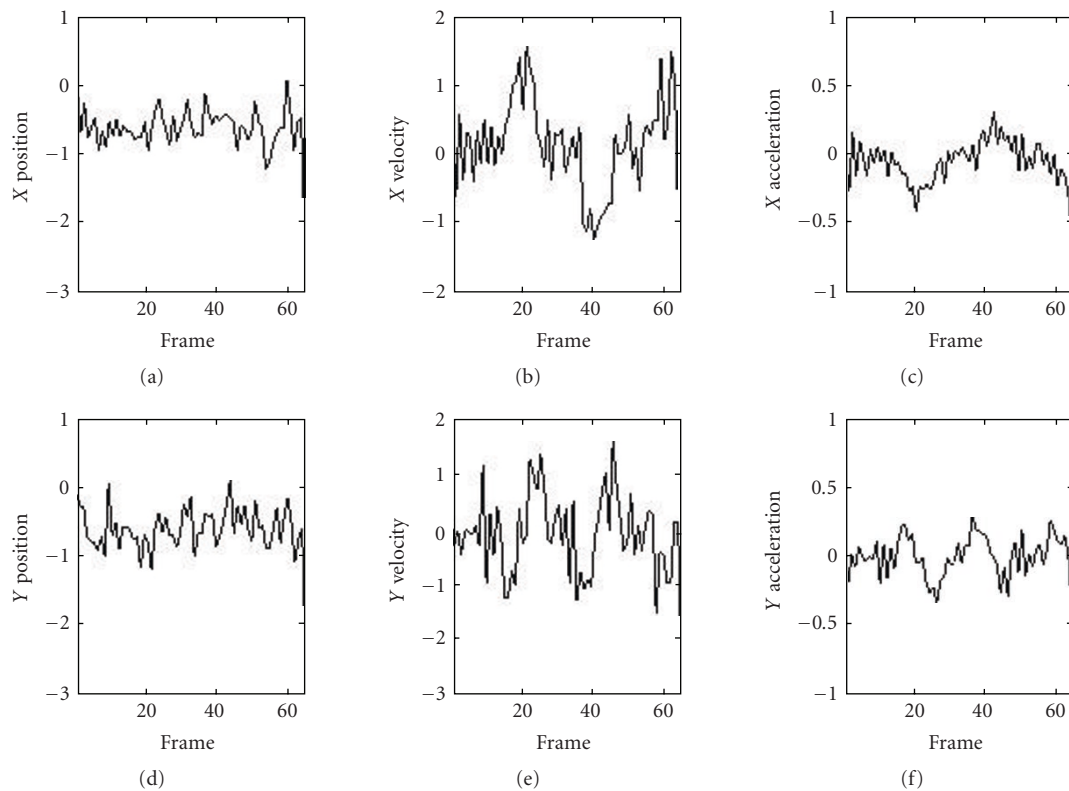\tag{A.11}
$$

which can be solved using Kalman filtering.

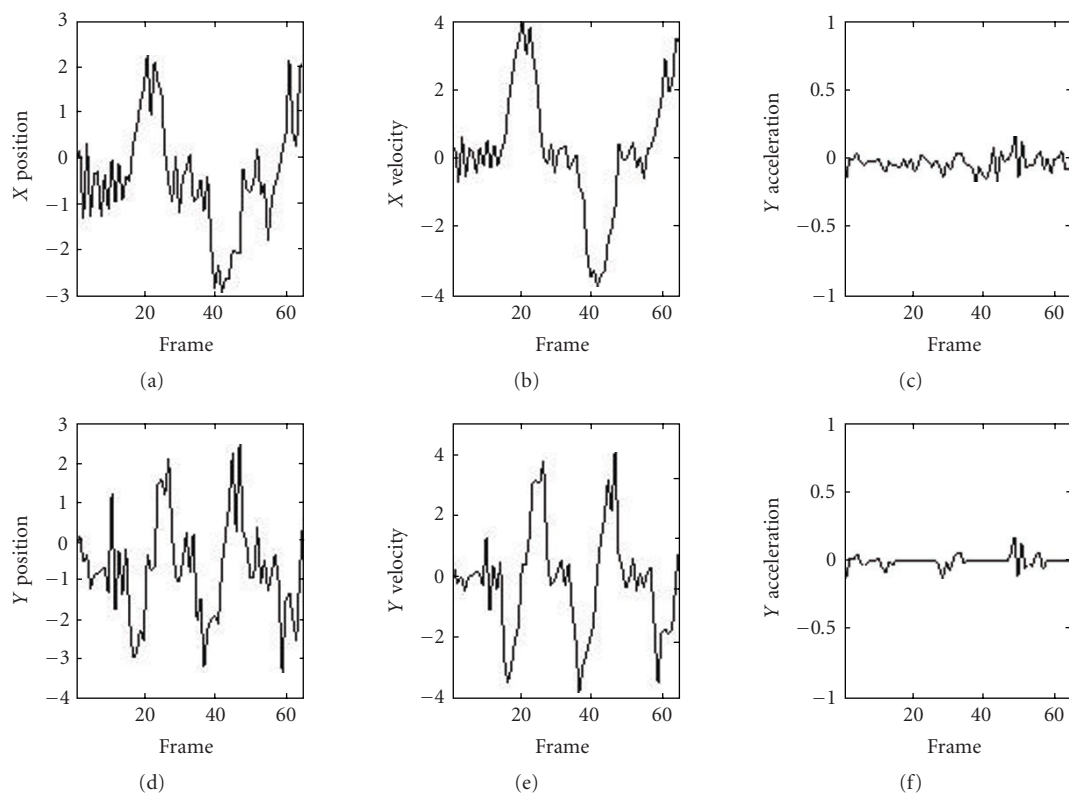Figure 15: Estimation error plot for all state parameters.

Figure 16: Prediction error plot for all state parameters.

REFERENCES

[1] Y. Bar-Shalom and T. E. Fortmann, *Tracking and Data Association*, Academic Press, San Diego, Calif, USA, 1988.

[2] S. Blackman and R. Popoli, *Design and Analysis of Modern Tracking Systems*, Artech House, Boston, Mass, USA, 1999.

[3] J. B. Pearson and E. B. Stear, "Kalman filter applications in airborne radar tracking," *IEEE Transactions on Aerospace and Electronic Systems*, vol. 10, no. 3, pp. 319–329, 1974.

[4] M. Farooq and S. Bruder, "Information type filters for tracking a maneuvering target," *IEEE Transactions on Aerospace and Electronic Systems*, vol. 26, no. 3, pp. 441–454, 1990.

[5] P. L. Bogler, "Tracking a maneuvering target using input estimation," *IEEE Transactions on Aerospace and Electronic Systems*, vol. 23, no. 3, pp. 298–310, 1987.

[6] K. Demirbas, "Manoeuvring-target tracking with the Viterbi algorithm in the presence of interference," *IEE Proceedings F: Radar and Signal Processing*, vol. 136, no. 6, pp. 262–268, 1989.

[7] T. C. Wang and P. K. Varshney, "A tracking algorithm for maneuvering targets," *IEEE Transactions on Aerospace and Electronic Systems*, vol. 29, no. 3, pp. 910–924, 1993.

[8] W.-R. Wu and D.-C. Chang, "Maneuvering target tracking with colored noise," *IEEE Transactions on Aerospace and Electronic Systems*, vol. 32, no. 4, pp. 1311–1320, 1996.

[9] J. R. Cloutier, C.-F. Lin, and C. Yang, "Enhanced variable dimension filter for maneuvering target tracking," *IEEE Transactions on Aerospace and Electronic Systems*, vol. 29, no. 3, pp. 786–797, 1993.

[10] D. Avitzour, "A maximum likelihood approach to data association," *IEEE Transactions on Aerospace and Electronic Systems*, vol. 28, no. 2, pp. 560–566, 1992.

[11] R. L. Streit and T. E. Luginbuhl, "Maximum likelihood method for probabilistic multihypothesis tracking," in *Signal and Data Processing of Small Targets*, vol. 2235 of *Proceedings of SPIE*, pp. 394–405, Orlando, Fla, USA, April 1994.

[12] H. Gauvrit, J. P. Le Cadre, and C. Jauffret, "A formulation of multitarget tracking as an incomplete data problem," *IEEE Transactions on Aerospace and Electronic Systems*, vol. 33, no. 4, pp. 1242–1257, 1997.

[13] A. Logothetis, V. Krishnamurthy, and J. Holst, "On maneuvering target tracking via the PMHT," in *Proceedings of the 36th IEEE Conference on Decision and Control*, vol. 5, pp. 5024–5029, San Diego, Calif, USA, December 1997.

[14] P. K. Willett, Y. Ruan, and R. L. Streit, "The PMHT for maneuvering targets," in *Signal and Data Processing of Small Targets*, vol. 3373 of *Proceedings of SPIE*, pp. 416–427, Orlando, Fla, USA, April 1998.

[15] P. Willett, Y. Ruan, and R. Streit, "PMHT: problems and some solutions," *IEEE Transactions on Aerospace and Electronic Systems*, vol. 38, no. 3, pp. 738–754, 2002.

[16] H. A. P. Blom and Y. Bar-Shalom, "The interacting multiple model algorithm for systems with Markovian switching coefficients," *IEEE Transactions on Automatic Control*, vol. 33, no. 8, pp. 780–783, 1988.

[17] G. A. Watson and W. D. Blair, "IMM algorithm for tracking targets that maneuver through coordinated turns," in *Signal and Data Processing of Small Targets*, vol. 1698 of *Proceedings of SPIE*, pp. 236–247, Orlando, Fla, USA, April 1992.

[18] M. T. Busch and S. S. Blackman, "Evaluation of IMM filtering for an air defense system application," in *Signal and Data Processing of Small Targets*, vol. 2561 of *Proceedings of SPIE*, pp. 435–447, San Diego, Calif, USA, July 1995.

[19] E. Mazor, A. Averbuch, Y. Bar-Shalom, and J. Dayan, "Interacting multiple model methods in target tracking: a survey," *IEEE Transactions on Aerospace and Electronic Systems*, vol. 34, no. 1, pp. 103–123, 1998.

[20] X. R. Li and Y. Zhang, "Numerically robust implementation of multiple-model algorithms," *IEEE Transactions on Aerospace and Electronic Systems*, vol. 36, no. 1, pp. 266–278, 2000.

[21] A. Jouan, E. Bossé, M.-A. Simard, and E. Shahbazian, "Comparison of various schema of filter adaptivity for the tracking of maneuvering targets," in *Signal and Data Processing of Small Targets*, vol. 3373 of *Proceedings of SPIE*, pp. 247–258, Orlando, Fla, USA, April 1998.

[22] T. Kirubarajan and Y. Bar-Shalom, "Kalman filter versus IMM estimator: when do we need the latter?" *IEEE Transactions on Aerospace and Electronic Systems*, vol. 39, no. 4, pp. 1452–1457, 2003.

[23] M. A. Zaveri, U. B. Desai, and S. N. Merchant, "PMHT based multiple point targets tracking using multiple models in infrared image sequence," in *Proceedings of the IEEE Conference on Advanced Video and Signal Based Surveillance (AVSS '03)*, pp. 73–78, Miami, Fla, USA, July 2003.

[24] G. J. McLachlan and T. Krishnan, *The EM Algorithm and Extensions*, John Wiley & Sons, New York, NY, USA, 1997.

[25] Y. Ruan and P. K. Willett, "Maneuvering PMHTs," in *Signal and Data Processing of Small Targets*, vol. 4473 of *Proceedings of SPIE*, pp. 186–197, San Diego, Calif, USA, July 2001.

[26] Y. Ruan and P. K. Willett, "Multiple model PMHT and its application to the second benchmark radar tracking problem," *IEEE Transactions on Aerospace and Electronic Systems*, vol. 40, no. 4, pp. 1337–1350, 2004.

[27] R. E. Helmick and G. A. Watson, "Interacting multiple model integrated probabilistic data association filters (IMM-IPDAF) for track formation on maneuvering targets in cluttered environments," in *Signal and Data Processing of Small Targets*, vol. 2235 of *Proceedings of SPIE*, pp. 460–471, Orlando, Fla, USA, April 1994.

[28] T. Kirubarajan, M. Yeddanapudi, Y. Bar-Shalom, and K. R. Pattipati, "Comparison of IMMPDA and IMM-assignment algorithms on real air traffic surveillance data," in *Signal and Data Processing of Small Targets*, vol. 2759 of *Proceedings of SPIE*, pp. 453–464, Orlando, Fla, USA, April 1996.

[29] F. Dufour and M. Mariton, "Tracking a 3D maneuvering target with passive sensors," *IEEE Transactions on Aerospace and Electronic Systems*, vol. 27, no. 4, pp. 725–739, 1991.

[30] S. S. Blackman, R. J. Dempster, and S. H. Roszkowski, "IMM/MHT applications to radar and IR multitarget tracking," in *Signal and Data Processing of Small Targets*, vol. 3163 of *Proceedings of SPIE*, pp. 429–439, San Diego, Calif, USA, July 1997.

[31] M. Hadzagic, H. Michalska, and A. Jouan, "IMM-JVC and IMM-JPDA for closely maneuvering targets," in *Proceedings of the 35th Asilomar Conference on Signals, Systems and Computers*, vol. 2, pp. 1278–1282, Pacific Grove, Calif, USA, November 2001.

[32] H. A. P. Blom and E. A. Bloem, "Combining IMM and JPDA for tracking multiple maneuvering targets in clutter," in *Proceedings of the 5th International Conference on Information Fusion*, vol. 1, pp. 705–712, Annapolis, Md, USA, July 2002.

[33] J. K. Tugnait, "Tracking of multiple maneuvering targets in clutter using multiple sensors, IMM, and JPDA coupled filtering," *IEEE Transactions on Aerospace and Electronic Systems*, vol. 40, no. 1, pp. 320–330, 2004.

[34] S. B. Colegrove and S. J. Davey, "PDAF with multiple clutter regions and target models," *IEEE Transactions on Aerospace and Electronic Systems*, vol. 39, no. 1, pp. 110–124, 2003.

[35] T. K. Moon, "The expectation-maximization algorithm," *IEEE Signal Processing Magazine*, vol. 13, no. 6, pp. 47–60, 1996.

[36] A. P. Dempster, N. M. Laird, and D. B. Rubin, "Maximum likelihood from incomplete data via the EM algorithm," *Journal of the Royal Statistical Society*, vol. 39, no. 1, pp. 1–38, 1977.

[37] S. T. More, A. A. Pandit, S. N. Merchant, and U. B. Desai, "Synthetic IR scene simulation of air-borne targets," in *Proceedings of the 3rd Indian Conference on Computer Vision, Graphics & Image Processing (ICVGIP '02)*, pp. 108–113, Ahmadabad, India, December 2002.

[38] M. A. Zaveri, S. N. Merchant, and U. B. Desai, "Multiple single pixel dim target detection in infrared image sequence," in *Proceedings of the International Symposium on Circuits and Systems (ISCAS '03)*, vol. 2, pp. 380–383, Bangkok, Thailand, May 2003.

[39] M. A. Zaveri, S. N. Merchant, and U. B. Desai, "Wavelet based detection and its application to tracking in IR sequence," to appear in *IEEE Transactions on Systems, Man, and Cybernetics, Part C: Applications and Reviews*.

[40] R. A. Singer, "Estimating optimal tracking filter performance for manned maneuvering targets," *IEEE Transactions on Aerospace and Electronic Systems*, vol. 6, no. 4, pp. 473–483, 1970.

[41] Y. Bar-Shalom, X. R. Li, and T. Kirubarajan, *Estimation with Applications to Tracking and Navigation*, John Wiley & Sons, New York, NY, USA, 2001.